J|A|C|S
ARTICLES
Published on Web 01/25/2003

Spectroscopic Characterization and Assignment of Reduction Potentials in the Tetraheme Cytochrome c_{554} from *Nitrosomonas Europaea*

Anup K. Upadhyay,[†] Doros T. Petasis,[†,§] Dave M. Arciero,[†] Alan B. Hooper,[‡] and Michael P. Hendrich*[,†]

Contributions from the Department of Chemistry, Carnegie Mellon University, Pittsburgh, Pennsylvania 15213 and the Department of Biochemistry, University of Minnesota, St. Paul, Minnesota 55108

Received July 8, 2002; E-mail: hendrich@andrew.cmu.edu

Abstract: The tetraheme cytochrome c_{554} (cyt c_{554}) from *Nitrosomonas europaea* is an essential electron transfer component in the biological oxidation of ammonia. The protein contains one 5-coordinate heme and three bis-His coordinated hemes in a 3D arrangement common to a newly characterized class of multiheme proteins. The ligand binding, electrochemical properties, and heme−heme interactions are investigated with Mössbauer and X- and Q-band (parallel/perpendicular mode) EPR spectroscopy. The results indicate that the 5-coordinate heme will not bind the common heme ligands, CN^-, F^-, CO, and NO in a wide pH range. Thus, cyt c_{554} functions only in electron transfer. Analysis of a series of electrochemically poised and chemically reduced samples allows assignment of reduction potentials for heme 1 through 4 of +47, +47, −147, and −276 mV, respectively. The spectroscopic results indicate that the hemes are weakly exchange-coupled ($J \approx -0.5$ cm^{-1}) in two separate pairs and in accordance with the structure: hemes 2/4 (high-spin/low-spin), hemes 1/3 (low-spin/low-spin). There is no evidence of exchange coupling between the pairs. A comparison of the reduction potentials between homologous hemes of cyt c_{554} and other members of this new class of multiheme proteins is discussed. Heme 1 has a unique axial N_δ-His coordination which contributes to a higher potential relative to the homologous hemes of hydroxylamine oxidoreductase (HAO) and the split-Soret cytochrome. Heme 2 is 300 mV more positive than heme 4 of HAO, which is attributed to hydroxide coordination to heme 4 of HAO.

Introduction

The autotrophic bacterium, *Nitrosomonas europaea*, derives energy for growth from the oxidation of ammonia to nitrite by the successive reactions of the membrane bound ammonia monooxygenase (AMO, $2H^+ + 2e^- + NH_3 + O_2 \rightarrow NH_2OH + H_2O$) and the soluble periplasmic hydroxylamine oxidoreductase (HAO, $NH_2OH + H_2O \rightarrow NO_2^- + 4e^- + 5H^+$).[1−4] The reducing equivalents generated in the HAO reaction are the starting point for essential electron transfer processes leading to a return of two electrons to the primary monooxygenase reaction and two electrons eventually to a terminal cytochrome c oxidase. The concomitantly generated proton gradient drives ATP synthesis. Hydrazine is also oxidized by HAO to nitrogen: $N_2H_4 \rightarrow N_2 + 4\ e^- + 4H^+$.[4,5] The physiological acceptor of electrons from HAO is the periplasmic cytochrome c_{554} (cyt c_{554}).[6−8] Electrons from cyt c_{554} are thought to pass through a membrane-anchored tetraheme cytochrome c_{M552} to ubiquinone and then to either AMO or the respiratory pathway.[9] In keeping with key roles in the energy yielding reactions of *Nitrosomonas*, the cellular concentrations of AMO, HAO, cyt c_{554}, and cytochrome aa_3 are within the same orders of magnitude.[10]

Cyt c_{554} is a monomeric protein (25 kDa) with a primarily α-helical structure containing four c-type hemes covalently bound via two cysteine thioether linkages in the −C−X−Y−C−H− sequence.[11] The histidine of the sequence is one of the axial ligands (proximal) to the heme. The heme organization of cyt c_{554} and the axial ligands from the crystal structure are

[†] Carnegie Mellon University.
[‡] University of Minnesota.
[§] Present address: Department of Physics, Allegheny College, Meadville, Pennsylvania 16335.

(1) Abbreviations: AMO, ammonia monooxygenase; HAO, hydroxylamine oxidoreductase; cyt, cytochrome; NiR, cytochrome c nitrite reductase; FRd, fumarate reductase; SSC, split-Soret cytochrome; EPR, electron paramagnetic resonance; CT, charge transfer; NHE, normal hydrogen electrode; HALS, highly anisotropic low-spin.

(2) Hooper, A. B.; Vannelli, T.; Bergmann, D. J.; Arciero, D. M. *Antonie van Leeuwenhoek* **1997**, *71*, 56−67.
(3) Wood, P. M., Prosser, J. I., Eds.; *Nitrification*; IRL Press: Oxford, U.K., 1986; pp 39−62.
(4) Hooper, A. B.; Nason, A. J. *J. Biol. Chem.* **1965**, *240*, 4044−4057.
(5) Anderson, J. H. *Biochem. J.* **1964**, *91*, 8−17.
(6) Yamanaka, T.; Shinra, M. *J. Biochem.* **1974**, *75*, 1265−1273.
(7) Arciero, D. M.; Balny, C.; Hooper, A. B. *Biochemistry* **1991**, *30*, 11466−11472.
(8) DiSpirito, A. A.; Taaffe, L. R.; Hooper, A. B. *Biochim. Biophys. Acta* **1985**, *806*, 320−330.
(9) Whittaker, M.; Bergmann, D.; Arciero, D.; Hooper, A. B. *Biochim. Biophys. Acta* **2000**, *1459*, 346−355.
(10) DiSpirito, A. A.; Taaffe, L. R.; Lipscomb, J. D.; Hooper, A. B. *Biochim. Biophys. Acta* **1985**, *827*, 320−326.
(11) Iverson, T. M.; Hendrich, M. P.; Arciero, D. M.; Hooper, A. B.; Rees, D. C. In *Handbook of Metalloproteins*; Messerschmidt, A., Huber, R., Poulos, T., Wieghardt, K., Eds.; John Wiley and Sons, Ltd: Chichester, U.K., 2001; pp 136−146.

10.1021/ja020922x CCC: $25.00

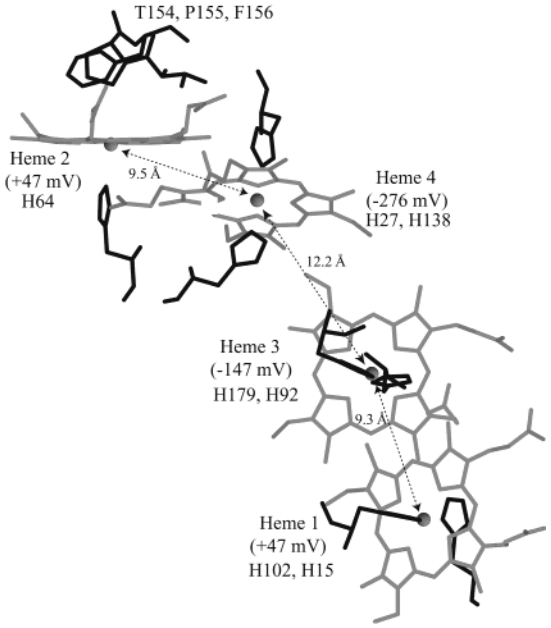

Figure 1. Structure of the heme array and axial histidine ligation in cyt c_{554} from crystals obtained from pH 10.1. The assignment of reduction potentials from this work is shown.

shown in Figure 1.[12,13] The numbering is based on heme position from the N-terminus, and the distances shown are between iron atoms. Hemes 1, 3, and 4 have bis-His axial coordination, whereas heme 2 is 5-coordinate with an axial His ligand. Cyt c_{554} belongs to a growing family of bacterial multiheme c-cytochromes which contain conserved structural arrangements of heme centers, despite significant differences in primary sequences and protein architecture. This family includes cyt c_{554},[12,13] HAO,[14] cytochrome c nitrite reductase (NiR),[15,16] fumarate reductase (FRd),[17−19] NapB,[20] and the split-Soret cytochrome (SSC).[21] Although cyt c_{554} is a tetraheme protein, it bears little resemblance to the well characterized tetraheme proteins cytochrome c_3[22] or the multiheme cytochrome subunit of photosynthetic reaction center.[23] HAO is the largest protein of this family, and each of the other proteins have regions of structure which align with HAO. For overlay pictures, see refs 13 and 20. Table 1 gives the correlation of the homologous hemes in the proteins which have the same structural arrangement. Three of the protein crystal structures show one 5-coordinate heme (noted in Table 1), while all other hemes have bis-His axial coordination.

Within the conserved structural domains of these proteins, there are three distinct, pairwise heme packing motifs. Two of these motifs show nearly parallel porphyrins which are offset. Examples of this occur between hemes 1 and 3 and hemes 2 and 4 of cyt c_{554}. The iron−iron distances for these pairs are 9.3 and 9.5 Å, respectively, and the porphyrin rings within each pair are in van der Waals contact. The third motif shows approximately perpendicular porphyrins with an iron−iron distance of 12.2 Å. This occurs between hemes 3 and 4 of cyt c_{554}, and this type of heme packing is also observed in cytochrome c_3.[22] All heme−heme packing motifs in the six proteins of Table 1 are represented by one of these three types.

The optical spectrum of cyt c_{554} exhibits a broad Soret band with a maximum at 407 nm from overlapping absorbances of the high- and low-spin hemes. The low-spin hemes exhibit a band with a maximum at 530 nm, and the high-spin heme exhibits a weak band at 645 nm.[24] Upon reduction, an α-band is observed at 554 nm and, thus, the name of the protein. The midpoint reduction potentials of the four hemes have been previously determined from optical studies and are +47, +47, −147, and −246 mV (vs NHE at pH 7).[25] The 5-coordinate heme II has been reported to be one of the two high-potential hemes with $E_m = +47$ mV.[7] The EPR spectrum of oxidized cyt c_{554} significantly differs from the spectra of isolated low- or high-spin heme centers. The main signal features occur at $g = 3.9$ and 2.0, resulting from some combination of spin-coupling between the hemes of cyt c_{554}. Mössbauer spectroscopy of oxidized cyt c_{554} determined that all iron is in the ferric state and that one heme is high-spin.[24] The zero-field Mössbauer spectrum at low temperature shows only quadrupole doublets and does not show the usual splitting from Fe^{3+} hyperfine interactions, which is a further indication of spin-coupling between the hemes. An NMR study of the oxidized protein also indicated the presence of one high-spin heme and more than one low-spin heme in the protein.[26]

In the present work, we have studied the ligand binding properties of cyt c_{554}. Since heme 2 is 5-coordinate, the possibility of ligand binding and a catalytic role has been considered. We show that none of the common heme ligands bind to cyt c_{554} in the oxidized or reduced states. Thus, we find no evidence for a function of cyt c_{554} other than electron transport. We have also studied the electrochemical properties of cyt c_{554} using EPR and Mössbauer spectroscopy on chemically reduced and electrochemically poised samples. Cyt c_{554} can be chemically reduced directly with sodium dithionite or by the native electron donor HAO.[7] We find that the midpoint potentials are consistent with the previous determinations from optical measurements.[25] New EPR and Mössbauer spectra are presented that allow differentiation and assignment of heme species. We are now able to assign the four reduction potentials to the specific hemes in the structure. The four hemes are not all spin-coupled together in a four heme cluster. Instead, in accordance with the structure, the hemes are spin-coupled in

(12) Iverson, T. M.; Arciero, D. M.; Barbara, T. H.; Logan, M. S. P.; Hooper, A. B.; Rees, D. C. *Nat. Struct. Biol.* **1998**, *5*, 1005−1012.
(13) Iverson, T. M.; Arciero, D. M.; Hooper, A. B.; Rees, D. C. *J. Biol. Inorg. Chem.* **2001**, *6*, 390−397.
(14) Igarashi, N.; Moriyama, H.; Fujiwara, T.; Fukumori, Y.; Tanaka, N. *Nat. Struct. Biol.* **1997**, *4*, 276−284.
(15) Einsle, O.; Messerschmidt, A.; Stach, P.; Bourenkov, G. P.; Bartunik, H. D.; Huber, R.; Kroneck, P. M. H. *Nature* **1999**, *400*, 476−480.
(16) Bamford, V. A.; Angove, H. C.; Seward, H. E.; Thomson, A. J.; Cole, J. A.; Butt, J. N.; Hemmings, A. M.; Richardson, D. J. *Biochemistry* **2002**, *41*, 2921−2931.
(17) Bamford, V.; Dobbin, P. S.; Richardson, D. J.; Hemmings, A. M. *Nat. Struct. Biol.* **1999**, *6*, 1104−1107.
(18) Taylor, P.; Pealing, S. L.; Reid, G. A.; Chapman, S. K.; Walkinshaw, M. D. *Nat. Struct. Biol.* **1999**, *6*, 1108−1112.
(19) Leys, D.; Tsapin, A. S.; Nealson, K. H.; Meyer, T. E.; Cusanovich, M. A.; Beeumen, J. J. V. *Nat. Struct. Biol.* **1999**, *6*, 1113−1117.
(20) Brigé, A.; Leys, D.; Meyer, T. E.; Cusanovich, M. A.; Van Beenmen, J. J. *Biochemistry* **2002**, *41*, 4827−4836.
(21) Matias, P. M.; Morais, J.; Coelho, A. V.; Meijers, R.; Gonzalez, A.; Thompson, A. W.; Sieker, L.; LeGall, J.; Carrondo, M. A. *J. Biol. Inorg. Chem.* **1997**, *2*, 507−514.
(22) Matias, P. M.; Morais, J.; Coelho, R.; Carrondo, M. A.; Wilson, K.; Dauter, Z.; Sieker, L. *Protein Sci.* **1996**, *5*, 1342−1354.
(23) Deisenhofer, J.; Epp, O.; Miki, K.; Huber, R.; Michel, H. *Nature* **1985**, *318*, 618−624.
(24) Andersson, K. K.; Lipscomb, J. D.; Valentine, M.; Münck, E.; Hooper, A. B. *J. Biol. Chem.* **1986**, *261*, 1126−1138.
(25) Arciero, D. M.; Collins, M. J.; Haladjian, J.; Bianco, P.; Hooper, A. B. *Biochemistry* **1991**, *30*, 11459−11465.
(26) Petersson, L.; Andersson, K. K. *Biochim. Biophys. Acta* **1987**, *915*, 261−266.

Table 1. Comparison of the Heme Packing Arrangements, Axial Histidine Plane Orientations, and Correlation of the Redox Potentials to the Crystal Structure

Protein	Heme Numbering[a]								Reference
			↓	↓	↓	↓			
Cyt c_{554}			$^{x}\mathbf{1}_{+47}$	$\mathbf{3}_{-147}$	$^{x}\mathbf{4}_{-276}$	$^{5}\mathbf{2}_{+47}$			12,13
HAO	**1**	**2**	$\mathbf{3}_{0}$	$\mathbf{5}_{0}$	$^{x}\mathbf{6}_{-190}$	$^{5}\mathbf{4}_{-260}$	$\mathbf{7}_{-150}$	**8**	14
NiR				$\mathbf{2}_{-37}$	$\mathbf{3}_{-107}$	$^{5}\mathbf{1}_{-107}$	$^{x}\mathbf{4}_{-323}$	$^{x}\mathbf{5}_{-323}$	15,16
SSC			$^{x}\mathbf{1}_{-168}$	$\mathbf{2}_{-330}$					21
FRd				**4**	$^{x}\mathbf{3}$		**2**	$^{x}\mathbf{1}$	17- 19
NapB			**1**	**2**					20

[a] The hemes are numbered according to their position from the N-terminus of the peptide sequence. The superscripts "5" or "x" denote the 5-coordinate hemes or bis-His axial coordination with crossed imidazole planes. All other hemes have approximately parallel bis-His axial coordination. Note that the 5-coordinate heme 1 in NiR has an axial Lys. The subscripts are the midpoint potentials (mV vs NHE). The following heme reduction potentials are not assigned yet: HAO (+288, −265, −412) and FRd (−238, −196, −146, −102). The brackets denote exchange-coupled hemes (except SSC and NapB). The numbering of hemes in FRd is stated as from the N-terminus,[19] but it appears to be actually from the C-terminus, which would explain the reversal of order relative to the other proteins.

two independent pairs; there is no detectable interaction between the two pairs. Finally, we compare the reduction potentials of the homologous hemes of this new class of multiheme proteins.

Materials and Methods

Purification of the Protein. The growth and ^{57}Fe enrichment of *Nitrosomonas europaea* and the purification of cyt c_{554} and HAO were performed as described previously.[25,27] All experiments were carried out in 50 mM potassium phosphate buffer pH 7.0, unless otherwise noted. The concentration of cyt c_{554} was determined spectrophotometrically with $\epsilon_{554} = 24.6\ mM^{-1}\ cm^{-1}$.[24] All chemicals were reagent grade or better. Doubly distilled or Millipore super Q water was used throughout.

Preparation of the Reduced Samples. Substrate induced reduction of cyt c_{554} by hydrazine (Sigma) was accomplished with excess hydrazine in the presence of a catalytic amount (3% molar ratio) of HAO. These samples will be referred to as "hydrazine/HAO poised" throughout the paper. The protein solutions were incubated for 10 minutes at room temperature before freezing in liquid nitrogen.

Electrochemical Titration. Samples of cyt c_{554} (3.8 mM) were poised at various potentials in the presence of mediators, following the procedure described previously.[25] The mediators were 1,2-naphthoquinone-4-sulfonic acid ($E_{m7} = +215$ mV), phenazine methosulfate ($E_{m7} = +80$ mV), gallocyanine ($E_{m7} = +21$ mV), pyocyanine ($E_{m7} = -34$ mV), indigo-5,5-disulfonic acid ($E_{m7} = -125$ mV), anthraquinone-2-sulfonic acid ($E_{m7} = -230$ mV), safranine O ($E_{m7} = -290$ mV), benzyl viologen ($E_{m7} = -350$ mV), and methyl viologen ($E_{m7} = -430$ mV). All the mediators were obtained from Aldrich or Sigma. The samples were equilibrated with the applied electrode potential for 2 h to complete the reduction.

EPR and Mössbauer Spectroscopy. X-band EPR spectra were acquired using a Bruker 300 spectrometer equipped with an Oxford ESR-910 liquid helium cryostat and a Bruker bimodal cavity. The quantification of all signals was relative to a CuEDTA spin standard. The spectra were obtained with a field modulation of $1mT_{pp}$ at 100 kHz unless otherwise noted. Parallel and perpendicular mode Q-band spectra were recorded on a Bruker 200 spectrometer with a home-built microwave probe and cryostat.[28] The temperature was calibrated using a carbon glass resistor (CGR-1-1000, Lake Shore Cryotronics). The magnetic field was calibrated with an NMR gaussmeter, and the microwave frequency was measured with a counter. The EPR simulation software was written by the authors.[29] The simulations are generated with consideration of all intensity factors, which allows computation of simulated spectra for a specified sample concentration. Mössbauer spectra were obtained on a constant acceleration instrument, and isomer shifts are reported with respect to an iron metal standard.

Results

Mössbauer Spectroscopy. The Mössbauer spectrum of fully oxidized cyt c_{554} recorded at 150 K (not shown) is similar to that observed in previous work at low temperature.[24] The spectrum contains doublets from four iron species, only one of which is resolved. The resolved doublet is from the high-spin Fe^{3+} heme 2 of the crystal structure, which is the only 5-coordinate heme in the protein.

The high-temperature Mössbauer spectrum of cyt c_{554} treated with a 2-fold excess of hydrazine in the presence of a catalytic amount of HAO (hydrazine/HAO poised, see Materials and Methods) is shown in Figure 2A. A control experiment with hydrazine in the absence of HAO showed no change from the oxidized spectrum, indicating that hydrazine does not react directly with cyt c_{554}. The solid line is a least-squares fit to the data with the parameters given in Table 2. Four doublets, each with $25 \pm 2\%$ of the total area, can be unambiguously assigned in this spectrum. The doublet marked II_R has parameters which are characteristic of high-spin Fe^{2+} heme. Since cyt c_{554} contains only one high-spin heme, this doublet is assigned to the reduced state of heme 2. The doublet marked I_R has parameters which are typical of a low-spin Fe^{2+} heme. We will demonstrate below from the EPR results that this doublet must originate from heme 1. The four absorbances associated with the remaining two doublets (labeled III_O, IV_O) must be arranged as an inner doublet and outer doublet to give similar isomer shifts and differing quadrupole splittings. The other arrangements of pairs would give hemes with isomer shifts of 0.03 and 0.32 mm/s, which are not in the standard range of values for low-spin hemes. The magnitude of the quadrupole splitting has been shown to be dependent on the relative orientation of the imidazole planes for bis-His axially coordinated hemes.[30−32] Parallel orientations

(27) Andersson, K. K.; Kent, T. A.; Lipscomb, J. D.; Hooper, A. B.; Münck, E. *J. Biol. Chem.* **1984**, *259*, 6833−6840.
(28) Petasis, D. T.; Hendrich, M. P. *J. Magn. Reson.* **1999**, *136*, 200−206.
(29) Hendrich, M. P.; Petasis, D.; Arciero, D. M.; Hooper, A. B. *J. Am. Chem. Soc.* **2001**, *123*, 2997−3005.
(30) Safo, M. K.; Gupta, G. P.; Watson, C. T.; Simonis, U.; Walker, F. A.; Scheidt, W. R. *J. Am. Chem. Soc.* **1992**, *114*, 7066−7075.

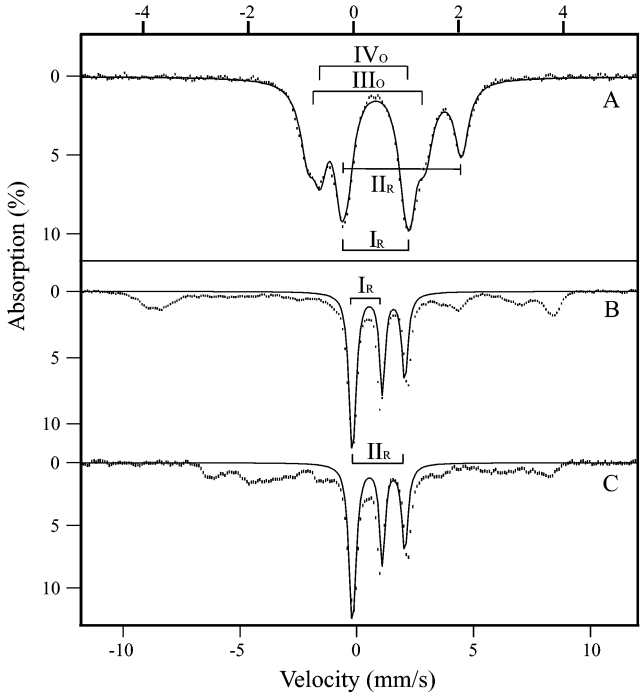

Figure 2. Mössbauer spectra of (A) hydrazine/HAO poised cyt c_{554} [1.7mM] pH 7.0, temperature 150 K, in absence of applied magnetic field. The solid line is a least-squares fit to the data with the parameters listed in Table 2. Each doublet is labeled by its respective heme species, where the subscript refers to either the oxidized (O) or reduced (R) state. Spectra at 4.2 K in (B) absence and (C) presence of a 45 mT magnetic field applied parallel to the incident γ radiation. The solid lines are generated for the doublets of I_R and II_R heme centers, each corresponding to 25% of the total area. The *x*-axis scale at the top is for part A, and the bottom, for parts B and C.

Table 2. Mössbauer and EPR Parameters of Cytochrome c_{554}[a]

sample	species	spin	δ (mm/s)	ΔE_Q (mm/s)	
oxidized	I_O	$^1/_2$	0.23(4)	2.0(1)	
	II_O	$^5/_2$	0.45(9)	1.3(2)	
	III_O	$^1/_2$	0.25(4)	2.2(1)	
	IV_O	$^1/_2$	0.17(4)	1.6(1)	
N_2H_4/HAO	I_R	0	0.42(4)	1.3(1)	
	II_R	2	0.98(4)	2.2(1)	
	III_O	$^1/_2$	0.25(4)	2.2(1)	$g = 3.24, 2.06, 1.10$
	IV_O	$^1/_2$	0.17(4)	1.6(1)	$g_{max} = 3.6$

[a] Mössbauer parameters at 150 K, $\Gamma = 0.34(3)$ mm/s. Subscripts "O" and "R" denote Fe^{3+} or Fe^{2+} species, respectively.

of imidazole planes give $\Delta E_Q > 2.0$ mm/s, whereas perpendicular orientations give $\Delta E_Q < 2.0$ mm/s. For cyt c_{554}, heme 3 has parallel imidazole planes and is thus assigned to doublet III_O with $\Delta E_Q = 2.2$ mm/s, whereas heme 4 has perpendicular imidazole planes and thus is assigned to doublet IV_O with $\Delta E_Q = 1.62$ mm/s. Addition of a large excess of hydrazine had no effect on the Mössbauer spectrum of Figure 2A, indicating that hydrazine/HAO poising reduces only hemes 1 and 2 of cyt c_{554} (half-reduced state).

With these parameters for the doublets of species III_O and IV_O, the doublets for species I_O and II_O can be determined from a fit of the oxidized spectrum (not shown) and are given in Table 2. The Mössbauer parameters determined for doublets I, III, and IV are typical of low-spin hemes, and that of II are typical of high-spin hemes.[33−35]

Mössbauer spectra of the hydrazine/HAO poised sample recorded at 4.2 K in the absence (Figure 2B) and presence (Figure 2C) of an applied magnetic field are also shown. As was noted in previous work, the lack of magnetic hyperfine features in the low-temperature spectrum of oxidized cyt c_{554} indicated magnetic interactions between all four hemes.[24] In contrast, the hydrazine/HAO poised sample at low temperature shows magnetic hyperfine features and nonmagnetic quadrupole doublets. The two doublets in Figure 2B and C, labeled I_R and II_R, are fit (solid line) with the same low-spin and high-spin Fe^{2+} species of Figure 2A, each having 25 ± 2% of the total area. In the presence of hydrazine, only two hemes are reduced, but the absorbances from all four hemes are affected. Thus, the magnetic hyperfine structure in Figure 2B and C must originate from species III_O and IV_O, which are both low-spin hemes ($S = {}^1/_2$). Furthermore, the magnetic spin systems within both diheme pairs, 1/3 and 2/4, must change upon reduction of two hemes to give two half-integer spin systems. Thus, one heme from each pair is reduced in the half-reduced state of the protein, rather than two hemes from the same pair.

In the next section, evidence will be presented for an interaction between species IV_O ($S = {}^1/_2$) and the reduced high-spin heme ($S = 2$); however, this interaction is not evident in the Mössbauer spectra at low magnetic field. For the case of a large, positive zero-field splitting (D) of the high-spin heme and a weak exchange interaction (J) with a low-spin heme, the spin expectations of the two sites are nearly unchanged from the expectations in the absence of the exchange interaction. Thus, the spectra of species II_R and IV_O are typical of the spectra of isolated hemes.

X-Band EPR Spectroscopy. The perpendicular ($\mathbf{B}_1 \perp \mathbf{B}$) and parallel mode ($\mathbf{B}_1 \parallel \mathbf{B}$) X-band EPR spectra of oxidized cyt c_{554} are shown in Figure 3. The perpendicular mode spectrum shows peaks at $g = 3.9$ and 2.7, a derivative feature at 2.06, and two valleys at 1.63 and 1.46. This spectrum matches that reported previously.[24,36] The parallel mode spectrum is new and shows signals at $g = 7.2$ and 3.2. The observation of a parallel mode signal for ferric hemes requires the presence of spin−spin interactions between hemes. In addition, the perpendicular mode signals are not typical of isolated hemes, indicating that all hemes in oxidized cyt c_{554} are spin-coupled, which is consistent with the Mössbauer data and previous conclusions.[24] The parallel mode signal resembles the parallel mode signals observed from the multiheme proteins NiR[16] and HAO.[37] However, the HAO signal is significantly weaker and shifted by 15 mT to higher field. The parallel mode signal from NiR is shifted by 25 mT lower in field than that of cyt c_{554}. Spin quantitation of these spectra using the double integration method is not possible, since these signals do not conform to an effective $S = {}^1/_2$ state.

The dashed lines in Figure 3 are spectra recorded at higher temperature. The intensity scale of all the spectra are multiplied

(31) Munro, O. Q.; Serth-Guzzo, J. A.; Turowska-Tyrk, I.; Mohanrao, K.; Shokhireva, T. K.; Walker, F. A.; Debrunner, P. G.; Scheidt, W. R. *J. Am. Chem. Soc.* **1999**, *121*, 11144−11155.
(32) Medhi, O. K.; Silver, J. *J. Chem. Soc., Dalton Trans.* **1990**, 555−559.
(33) Debrunner, P. G. In *Iron Porphyrins*; Lever, A., Gray, H., Eds.; VCH Publishers: New York, 1989; Part 3, pp 137−234.
(34) Münck, E. In *Physical Methods in Bioinorganic Chemistry*; Que, L., Jr., Ed.; University Science Books: Sausalito, CA, 2000; pp 287−319.
(35) Gütlich, P.; Link, R.; Trautwein, A. *Mössbauer Spectroscopy and Transition Metal Chemistry*; Springer-Verlag: Berlin, 1979.
(36) Andersson, K. K.; Lipscomb, J. D.; Hooper, A. B. *Inorg. Chim. Acta* **1983**, *79*, 181−182.

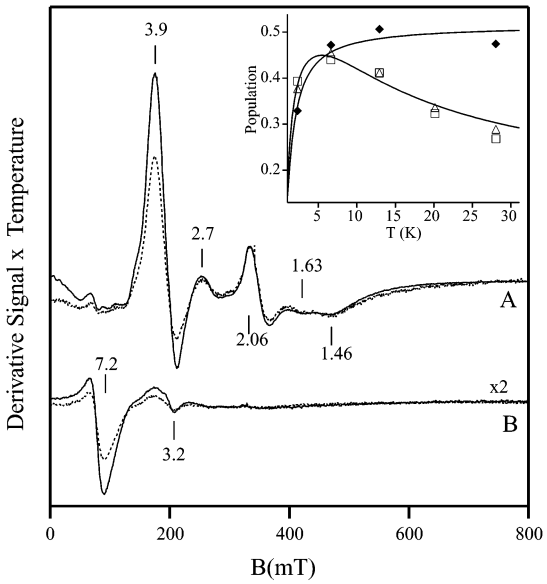

Figure 3. X-band EPR spectra of oxidized cyt c_{554} [1 mM] pH 7.0 for (A) $\mathbf{B}_1 \perp \mathbf{B}$ and (B) $\mathbf{B}_1 \parallel \mathbf{B}$. The spectra are plotted as signal intensity times temperature. The sample temperature was 7 K (solid lines) and 28 K (dashed lines). The vertical scale of B is magnified by ×2. Microwave frequency, 9.62 (A), 9.24 GHz (B); microwave power, 0.2 mW. The inset shows the signal times temperature dependence for the $g = 7.2$ (△), 3.9 (□), and 2.06 (◆) signals.

by temperature, thus signal intensities that are Curie Law dependent ($\sim 1/T$) will not change as a function of temperature. Figure 3 demonstrates that the signals at $g = 2.7$, 2.06, 1.63, and 1.46 originate from a spin system separate from that of the $g = 3.9$ and the $\mathbf{B}_1 \parallel \mathbf{B}$ signals. The signal time temperature dependence of the signals at $g = 7.2$ (triangles), 3.9 (squares), and 2.06 (diamonds) is shown in the inset. An exchange interaction between two $S = {}^1/_2$ low-spin heme centers is expected to give system spin states which are approximately represented by a singlet and triplet. For an antiferromagnetic interaction, the triplet state will be $2J$ higher in energy than the singlet state ($H = -2J\mathbf{S}_1 \cdot \mathbf{S}_2$). The curve shown in the inset on the data for the $g = 2.06$ signal is the population of a doublet within the triplet state for $J = -0.7(5)$ cm^{-1}. The signal deviates from Curie Law at low temperature because of depopulation of the triplet state. Thus, a pair of low-spin hemes exhibits a weak antiferromagnetic exchange interaction.

An exchange interaction between high-spin and low-spin ferric hemes would result in system spin states of $S = 2$ and 3 for $|J| \gg |D|$, where D is the axial splitting parameter of the high-spin heme. However, the X-band spectra, and Q-band spectra to follow, do not show signals that can be assigned to such system spin states. For $|J| \ll |D|$, the exchange interaction of the low-spin heme results in the formation of isolated quartets of spin levels that originate from the $m_s = \pm {}^1/_2$, $\pm {}^3/_2$, and $\pm {}^5/_2$ doublets of the high-spin heme. The curve shown in the inset on the data for the $g = 7.2$ and 3.9 signals is the population of the first and second excited states of the lowest lying quartet. The curve is calculated for $H = -2J\mathbf{S}_1 \cdot \mathbf{S}_2 + D(S_{1z}^2 - {}^{35}/_{12})$, where $S_1 = {}^5/_2$, $S_2 = {}^1/_2$, $J = -0.4(2)$ cm^{-1}, and $D = 7(2)$ cm^{-1}. Thus, this pair also exhibits a weak antiferromagnetic exchange interaction. The D-value is consistent with that expected for a ferric high-spin heme.[33] Currently, we cannot rule out that the signals originate from one of the other two excited transitions within the lowest quartet. However, this ambiguity does not significantly alter the results and is accounted for in the stated uncertainties of the values of J and D.

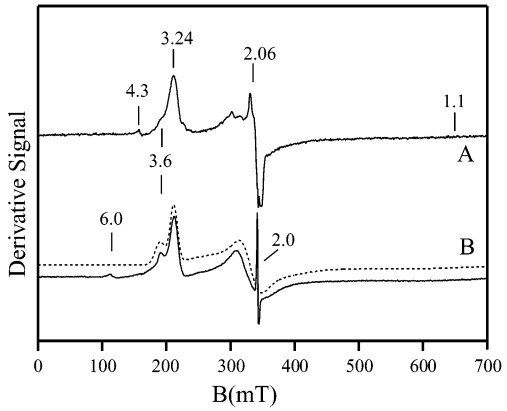

Figure 4. X-band EPR spectra ($\mathbf{B}_1 \perp \mathbf{B}$) of cyt c_{554} [1 mM] pH 7.0. (A) Hydrazine/HAO poised. (B) Electrochemically poised at −50 mV. The dashed line is a quantitative simulation for two independent $S = {}^1/_2$ species at concentrations both equal to the protein concentration, with $g_1 = 3.24$, 2.06, and 1.10 and $g_2 = 3.6$, 2.0, and 0.62. The signals at $g = 4.3$ and 6 are from Fe^{3+} species of less than 3% of the protein concentration. Experimental conditions: temperature 15K; frequency, 9.62 GHz; power, 0.2 mW.

The perpendicular mode EPR spectrum of hydrazine/HAO poised cyt c_{554} is shown in Figure 4A. The spectrum shows a set of g-values at 3.24, 2.06, and 1.1 (broad) and a shoulder at $g = 3.6$. The parallel mode signal vanishes under these conditions. The signal at $g = 4.3$ is from an Fe^{3+} impurity, and the sharp feature at $g = 2.06$ is from a Cu^{2+} impurity; both quantitate to less than 3% of the protein concentration. Figure 4B shows the spectrum of a sample of cyt c_{554} which was electrochemically poised at −50 mV versus NHE. For this sample, the two hemes with $E_m = +47$ mV are fully reduced and the hemes with $E_m = -147$ mV and −276 mV are fully oxidized. This spectrum looks essentially the same as the hydrazine/HAO poised spectrum. The sharp peak at $g = 2$ (Figure 4B) is a minority radical species from a reduction mediator. The small peak at $g = 6.0$ is from a high-spin Fe^{3+} species of less than 2% of the total iron. The dashed line above Figure 4B is a quantitative simulation for two $S = {}^1/_2$ species with $g = 3.24$, 2.06, and 1.1 and $g = 3.6$, 2.0, and 0.6. We label these species III_O and IV_O, respectively. The intensity of the simulation is determined by the protein concentration and matches the experimental spectrum. Thus, species III_O and IV_O both have 1 to 1 stoichiometry with protein concentration, and the hydrazine/HAO poising results in two hemes reduced (half-reduced state). These are the same two species that were identified in the Mössbauer spectra. The g-values 3.24, 2.06, and 1.1 of species III_O are typical of low-spin Fe^{3+} heme with bis-His axial coordination. The ligand field parameters calculated from the g-values are $|\Delta/\lambda| = 2.39$ and $|V/\Delta| = 1.02$.[38] The signal from species IV_O with $g_{max} = 3.6$ (shoulder) is typical of a large g_{max} signal, also called a HALS type heme.[39−44] The

(37) Hendrich, M. P.; Logan, M.; Andersson, K. K.; Arciero, D. M.; Lipscomb, J. D.; Hooper, A. B. *J. Am. Chem. Soc.* **1994**, *116*, 11961−11968.
(38) Blumberg, W. E.; Peisach, J. *Adv. Chem. Ser.* **1971**, *100*, 271−291.
(39) Walker, F. A.; Huynh, B. H.; Scheidt, W. R.; Osvath, S. R. *J. Am. Chem. Soc.* **1986**, *108*, 5288−5297.
(40) Safo, M. K.; Gupta, G. P.; Walker, F. A.; Scheidt, W. R. *J. Am. Chem. Soc.* **1991**, *113*, 5497−5510.
(41) Shokhirev, N. V.; Walker, F. A. *J. Am. Chem. Soc.* **1998**, *120*, 981−990.
(42) Berry, M. J.; George, S. J. Thomson, A. J.; Santos, H.; Turner, D. L. *Biochem J.* **1990**, *270*, 413−417.
(43) Salerno, J. C. *Biochem. Soc. Trans.* **1985**, *13*, 611−615.
(44) Palmer, G. *Biochem. Soc. Trans.* **1985**, *13*, 548−560.

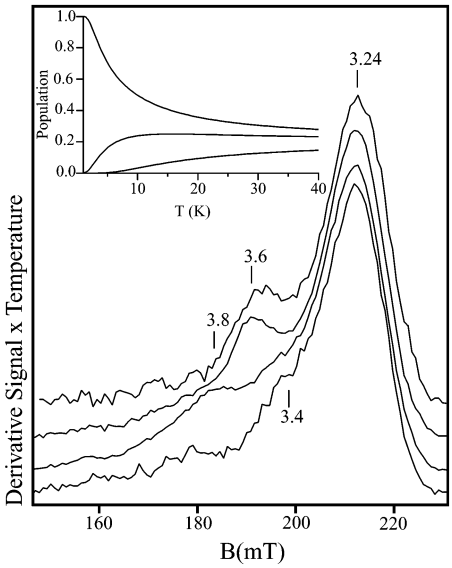

Figure 5. X-band EPR spectra ($\mathbf{B}_1 \perp \mathbf{B}$) of hydrazine/HAO poised cyt c_{554} recorded at temperatures of 2, 6, 16, and 35 K (bottom to top, respectively). All the spectra have been multiplied by the corresponding temperature to show the Curie Law temperature dependence of the $g = 3.24$ signal. Experimental conditions same as Figure 4. See text for explanation of inset.

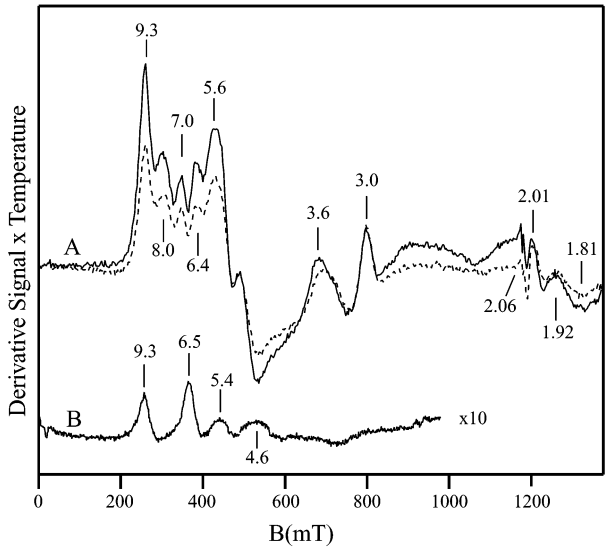

Figure 6. Q-band EPR spectra of oxidized cyt c_{554} [7.5 mM] pH 7.0 for (A) $\mathbf{B}_1 \perp \mathbf{B}$ and (B) $\mathbf{B}_1 \parallel \mathbf{B}$. The spectra are plotted as signal intensity times temperature. The sample temperature was 7 K (solid lines) and 31 K (dashed line). Microwave frequency, 34.0 GHz; power: 0.05 mW (A) and 0.5 mW (B).

two lower *g*-values of this species cannot be determined from the data but are assumed values in order to show that the concentration of this species is consistent with one center per protein. The lower intensity of the $g_{max} = 3.6$ signal compared to the $g = 3.24$ signal is due to the broader line shape of the large g_{max} signal.

The signal times temperature dependence of the EPR signal of half-reduced cyt c_{554} is shown in Figure 5 for temperatures 2 to 35 K. For such a plot, signal intensities that are Curie law dependent will be independent of temperature. Figure 5 shows that the signal at $g = 3.6$ from species IV_O shifts between $g = 3.4$ and 3.8 as a function of temperature, but the other strong signal at $g = 3.24$ from species III_O does not change with temperature. Thus, the $g = 3.24$ signal from species III_O originates from a simple $S = {}^1/_2$ paramagnetic center; however the $g = 3.6$ signal has a more complicated temperature dependence indicative of an interaction with another spin center. As described above, the ferric high-spin heme is exchange-coupled to a ferric low-spin heme. In the reduced sample, we suspect the ferrous high-spin heme is also weakly ($J \ll D$) spin-coupled to a ferric low-spin heme. The ground $m_s = 0$ state of the $S = 2$ manifold of the high-spin ferrous heme splits into a doublet which retains the properties of the $S = {}^1/_2$ doublet of the ferric low-spin heme. The $m_s = \pm 1$ and ± 2 doublets of the $S = 2$ manifold each split into quartets and are at higher energies for $D > 0$. The inset of Figure 5 shows the population versus temperature of doublets which originate from the $m_s = 0, \pm 1$, and ± 2 states of the high-spin ferrous heme (top to bottom, respectively). The curves are calculated for $H = -2J\mathbf{S}_1 \cdot \mathbf{S}_2 + D(S_{1z}^2 - 2)$ with $S_1 = 2$, $S_2 = {}^1/_2$, $D = 5\ cm^{-1}$, and $J/D = 0.1$. The *D*-value is assumed from literature values for ferrous high-spin hemes.[33] At 2 K, the ground doublet is mainly populated and the signal reflects the properties of species IV_O, as if it were not exchange-coupled. At 6 K and above, a significant population of excited doublets occurs which may explain the observed signal changes. The resolution of the signal is too low to make definite assignments; however, the signal changes for species IV_O as a function of temperature suggest an interaction between the ferrous high-spin heme and a ferric low-spin heme.

Q-Band EPR Spectroscopy. Figure 6 shows Q-band (34 GHz) EPR spectra of oxidized cyt c_{554} for perpendicular ($\mathbf{B}_1 \perp \mathbf{B}$) and parallel ($\mathbf{B}_1 \parallel \mathbf{B}$) microwave orientations. As with the X-band spectra, because of spin-coupling between the hemes, the Q-band spectra are not typical of isolated heme signals. The dashed line in Figure 6A shows the spectra at higher temperature, plotted as signal times temperature. The signals for $g > 4$ show a decrease in intensity at higher temperature, indicating depopulation of the associated spin manifold. The temperature dependence of the $g > 4$ signals is the same as that of the X-band signal at $g = 3.6$ in Figure 3. Thus, these signals are associated with the exchange-coupled high-spin/low-spin heme pair. The signal-to-noise of the parallel mode signal is too low to make an assignment. The signal at $g = 3.0$ in Figure 6A has the same temperature dependence as the X-band signal at $g = 2.06$ of Figure 3. Thus, this signal is associated with the exchange-coupled low-spin/low-spin heme pair. The temperature dependence of the $g = 3.6$ signal is more complicated and may have contributions from both spin systems. A full understanding of these spectra is beyond the scope of the present work. However, the features in Figure 6A with $g > 4$ are suggestive of a high-spin Fe^{3+} center. The typical high-spin heme signals, which would be centered around $g = 6$, are apparently split and shifted because of the weak spin exchange interaction with the low-spin heme.

Hydrazine/HAO poised samples of cyt c_{554} resulted in the loss of all signals observed in Figure 6. The resulting Q-band spectrum (not shown) has features at the same *g*-values as the X-band spectrum, which is consistent with reduction of two hemes, one from each pair.

Assignment of Species to Hemes of Structure. The four hemes of cyt c_{554} are structurally arranged in two pairs: 1/3 and 2/4.[12,13] The Fe−Fe distances are shown in Figure 1, the plane-to-plane distance within each pair is approximately

3.7 Å and the distance between pairs (heme 3−4) is 6 Å. From the above results, we are now able to make specific assignments of the spectroscopic species to the hemes of the crystal structure.

The crystal structure of the protein[12,13] shows that only heme 2 is 5-coordinate, and thus, it must be associated with the only high-spin center, species II. The structure shows that both hemes 1 and 4 have axial bis-His coordination in which the imidazole planes are perpendicular. This crossed axial imidazole geometry has been shown to give a large g_{max} EPR signal for low-spin Fe^{3+} hemes.[30,39−41] Heme 3, in contrast, has nearly parallel imidazole planes and thus must have *g*-values of a typical bis-His heme center. Since heme 3 is the only such heme, and only species III_O has such a set of typical low-spin *g*-values, we assign species III_O to the oxidized state of heme 3. For the next assignment, we note that the EPR and Mössbauer signals from both heme pairs are affected upon hydrazine/HAO poising. In this half-reduced sample, heme 3 remains oxidized. Thus, to affect change in the heme pair 1/3, heme 1 must be reduced in the half-reduced samples. This allows us to assign the Mössbauer doublets I_O and I_R to the oxidized and reduced states of heme 1. Finally, hemes 1 and 2 are both reduced in the half-reduced sample and thus give no EPR signals. As just stated, the oxidized state of heme 3 gives species III_O with $g = 3.24$, 2.06, and 1.10 of Figure 4. Species IV_O of Figure 4 with $g_{max} = 3.6$ must, by elimination, originate from the oxidized state of heme 4. This assignment is consistent with the fact that heme 4 has axial histidines with perpendicular imidazole planes and must therefore have $g_{max} > 3.4$. Furthermore, these assignments are consistent with the observation in the half-reduced sample that species IV_O (heme 4) is spin-coupled to the reduced high-spin heme (heme 2).

Electrochemical Titration. The X-band EPR spectra of cyt c_{554} electrochemically poised at different potentials are shown in Figure 7 for $\mathbf{B}_1 \perp \mathbf{B}$ (solid lines) and $\mathbf{B}_1 \parallel \mathbf{B}$ (dashed lines). Figure 7A shows spectra of the sample poised at $E_m = +202$ mV versus NHE. The spectra are essentially that of the oxidized sample (Figure 3). The sharp signal at $g = 2$ is from the mediators used for transferring electrons from the electrode to the protein. As the sample potential is lowered to +65 mV (Figure 7B) and +30 mV (Figure 7C), all signals from the oxidized state of the sample progressively lose intensity and are replaced by signals observed from the hydrazine/HAO poised sample. For Figure 7D, the sample is poised at −50 mV. The $g = 3.9$ and $\mathbf{B}_1 \parallel \mathbf{B}$ signals have nearly vanished, and the resulting $\mathbf{B}_1 \perp \mathbf{B}$ spectrum is similar to the half-reduced spectrum of the protein of Figure 4. The intensity of the oxidized signals as a function of reduction potential gives a midpoint potential of approximately +50 mV, on the basis of the Nernst equation. The loss of the signals correlates to the reduction of hemes 1 and 2. These results are found to be in agreement with the previous finding of two hemes in cyt c_{554} with $E_m = +47$ mV.[25] Figure 7E shows the spectrum of cyt c_{554} poised at −225 mV. At this potential, the two hemes with $E_m = +47$ mV and 95% of the −147 mV heme should be reduced. Consistent with these potentials, Figure 7E shows a signal from only one oxidized heme species at $g = 3.6$. Consequently, the heme species with $g = 3.24$, 2.06, and 1.10, which is from heme 3, must have the corresponding midpoint potential of −147 mV. The heme species remaining in Figure 7E with $g = 3.6$, which is from heme 4, must have the corresponding midpoint potential of −276 mV. Consistent with the −276 mV assignment, the $g = 3.6$ signal vanishes for a sample poised at −310 mV (not shown). The midpoint potentials observed here with EPR spectroscopy at low temperature are consistent with those obtained from optical spectroscopy at room temperature. This titration allows the assignments of the spectroscopic species to specific potentials, and in turn, to specific hemes of the structure, as shown in Figure 1.

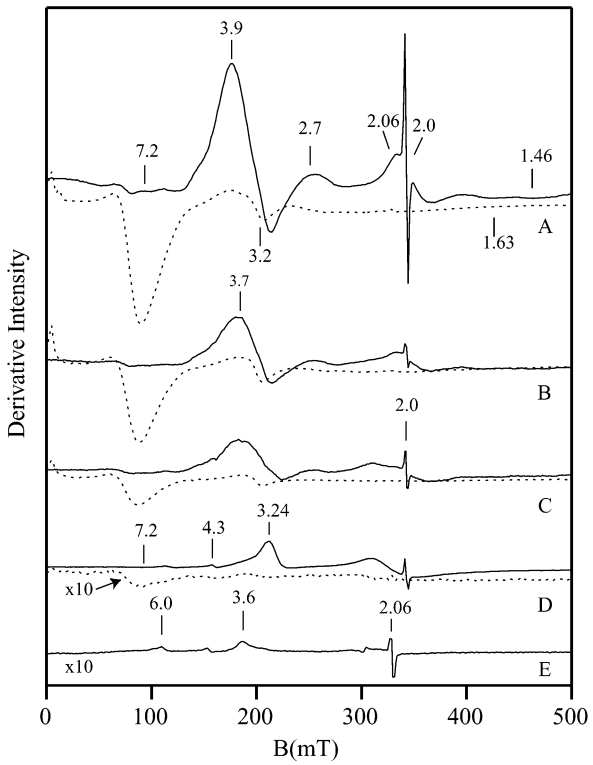

Figure 7. X-band EPR spectra of electrochemically poised samples of cyt c_{554} [3.8 mM] pH 7.0 for $\mathbf{B}_1 \perp \mathbf{B}$ (solid lines) and $\mathbf{B}_1 \parallel \mathbf{B}$ (dashed lines). The electrode potentials (vs NHE) are (A) +202 mV, (B) +65 mV, (C) +30 mV, (D) −50 mV, (E) −225 mV. Part E and $\mathbf{B}_1 \parallel \mathbf{B}$ in part D are displayed at ×10 magnification. Experimental conditions: temperature, 15 K ($\mathbf{B}_1 \perp \mathbf{B}$) and 2 K ($\mathbf{B}_1 \parallel \mathbf{B}$); frequency, 9.62 GHz ($\mathbf{B}_1 \perp \mathbf{B}$) and 9.24 GHz ($\mathbf{B}_1 \parallel \mathbf{B}$); microwave power, 0.2 mW.

Ligand Binding. We have studied the ligand binding properties of oxidized cyt c_{554} at pH 7.0 with a large excess of CN^-, CO, NO, and F^- as potential ligands. The spectra recorded on those protein samples showed no change, indicating that the protein does not bind any of these molecules or ions at neutral pH. Considering the possibility that cyt c_{554} may bind NO in the reduced state, as observed for NiR[45] and HAO,[46] we incubated a dithionite reduced sample at pH 7 with an excess of NO gas under anaerobic conditions. The EPR spectrum of the reduced sample before NO addition showed no significant signals. The EPR spectrum of the NO treated sample showed very weak signals identical to oxidized protein and a small signal near $g = 1.98$ from excess NO present in the solution. If NO binds to a ferrous heme, we would expect to see a low-spin $S = {}^1/_2$ signal, which would easily be observed over the background of weak signals. However, no new signal was observed that could be attributed to a low-spin Fe^{2+} heme−

(45) Stach, P.; Einsle, O.; Schumacher, W.; Kurun, E.; Kroneck, P. M. H. *J. Inorg. Biochem.* **2000**, *79*, 381−385.
(46) Hendrich. M. P.; Upadhyay, A. K.; Riga, J.; Arciero, D. M.; Hooper, A. B. *Biochemistry* **2002**, *41*, 4603−4611.

NO complex, indicating that NO does not bind to reduced cyt c_{554}. Thus, unlike the 5-coordinate hemes of NiR and HAO, the 5-coordinate heme 2 in cyt c_{554} does not bind ligands in either the reduced or oxidized states.

We have also examined the possibility of ligand binding in alkaline (pH 10) medium. A cyt c_{554} sample was prepared in 100 mM KPi at pH 10 and was treated with a 100 fold excess of F^-. Spectra recorded on this sample show no change from the oxidized spectrum even after incubating the reaction mixture for 1 h at room temperature. The sample prepared at higher pH 10.6 shows signals at $g = 6$ from a high-spin heme species and at $g = 2.9$, 2.3, and 1.4 from a low-spin species. In addition to the above new signals, the $g = 3.9$ signal loses intensity and develops a shoulder near $g = 3.5$. The high pH sample also shows a sharp signal at $g = 4.3$. Similar results were observed in acidic medium at pH 4.0. The presence of new signals at $g = 6$ and 4.3 suggest changes in the heme−heme interactions consistent with denaturation of the protein at these extreme nonphysiological conditions.

Discussion

Heme−Heme Interactions. In the fully oxidized state of the protein, there are two separate spin-coupled heme pairs. Hemes 1 and 3 are both low-spin ($S = 1/2$) and display a weak antiferromagnetic exchange coupling, $J = -0.7(5)$ cm^{-1}. Hemes 2 and 4 are $S = {}^5/_2$ and ${}^1/_2$, respectively, and also display a weak antiferromagnetic exchange coupling, $J = -0.4(2)$ cm^{-1}. There is no evidence for a spin interaction between the pairs. The EPR signals display separate sets of signals with differing temperature dependences that can be associated with the two specific pairs. In addition, the half-reduced state of the protein shows that heme 3 and heme 4 are not interacting. Thus, all 4 hemes are not part of the same exchange-coupled spin cluster. These observations are consistent with the crystal structure which shows a pairwise grouping of heme, with a longer distance between the pairs. The crystal structure of cyt c_{554} does not show a covalent pathway which might serve as a conduit for these exchange interactions; however, similar weak exchange interactions were first observed for the structurally similar heme pairs of HAO.[29] In that work, it was concluded that the exchange interactions in HAO originate from an edge-to-edge overlap of porphyrin orbitals, and we suggest the same occurs in cyt c_{554}. The values of the exchange couplings determined here are consistent with the report from previous Mössbauer results that all hemes appear to be decoupled in a magnetic field of 6 T.[24] At this field, the spin expectations of all four heme centers are approximately equal to the expectations in the absence of an exchange interaction.

Consistent with the structural assignments, the $g = 3.9$ (X-band) resonance is also observed in NiR which contains a homologous high-spin/low-spin heme pair, $1/3_{NiR}$.[16,47,48] Moreover, the $g = 3.9$ (X-band) and $g > 4$ (Q-band) signals are not observed from HAO, since for the homologous heme pair, $4/6_{HAO}$, both hemes are low-spin.[29] Interestingly, the only heme in HAO with crossed imidazole planes is heme 6_{HAO}, and this heme aligns with heme 4_{c554}, which also has crossed imidazoles. We have recently detected a signal from heme 6_{HAO} by removing the spin-coupling to heme 4_{HAO} with NO addition.[46] NO binds to heme 4_{HAO} and changes its spin state to $S = 0$. An EPR signal from heme 6_{HAO} alone is then observed to have $g_{max} = 3.4$, which is similar to that observed here for heme 4_{c554} with a g_{max} of 3.6. Both g_{max}-values are consistent with the crossed imidazole configuration.

Protein Function. The 5-coordinate heme 2 of cyt c_{554} does not bind small ligands that would typically coordinate to hemes in either the oxidized or reduced states. This is consistent with an electron transfer function, rather than substrate binding and catalysis. A previous study observed the binding of small ligands in acidic conditions.[24] We suspect that binding only occurs under denaturing conditions. Here, we observe no ligation changes in the pH range 4−10. Beyond this pH range, new signals are observed at $g = 6$ from hemes which are likely a result of some protein denaturation. The crystal structure to 1.6 Å resolution indicates that heme 2 is well shielded from binding an exogenous ligand by the presence of three amino acid residues Thr 154, Pro 155, and Phe 156.[12,13] Large concentrations of the smallest ligand F^- did not affect the spectra, indicating that these protein residues quite effectively shield the open coordination site from all solvent molecules. This would be appropriate for an electron transfer site; otherwise, its reduction potential would be perturbed by solvent binding at the iron. The 5-coordinate heme 2 site of cyt c_{554} is unique in protein structure. Type II cytochrome c-hemes (cytochrome c′) are also 5-coordinate and high-spin. However, these hemes are found in a classic four antiparallel α-helical bundle structure which has no similarity to cyt c_{554}.[49,50]

Comparison of the Reduction Potentials of the Hemes in Cyt c_{554} with Homologous Hemes of Multiheme Proteins. A comparison of the relative heme arrangements and assigned reduction potentials of six multiheme proteins are given in Table 1. Despite having similar 3-dimensional arrangements, the reduction potentials of the hemes are quite different. A comparison may provide insight for an understanding of the regulation of reduction potentials in heme proteins. We comment on five types of interactions which affect heme potentials: Fe−N_{axial} bond length, H-bonding to axial His, axial His plane orientation, H-bonding to heme propionates, and solvent accessibility. Perpendicular axial bis-His orientation has been suggested to contribute a +50 mV shift versus parallel orientation.[39] Solvent interactions leading to stabilization of the negative charge on the heme propionates contributes a shift of about −30 mV, while neutralization of the charge on the solvent exposed heme propionates by H-bonding with the positively charged peptide residues contributes approximately a +40 mV shift.[51] Increasing solvent exposure to hemes can result in a substantial lowering of the iron potentials.[52−54]

The four hemes of cyt c_{554} (1 to 4) are arranged in an identical stacking motif with four hemes of HAO (3 to 6, respectively). Except for the hemes with only one coordinating His (heme

(47) Schumacher, W.; Hole, U.; Kroneck, P. M. H. *Biochem. Biophys. Res. Commun.* **1994**, *205*, 911−916.
(48) Costa, C.; Moura, J. J. G.; Moura, I.; Liu, M. Y.; Peck, H. D., Jr.; LeGall, J.; Wang, Y.; Huynh, H. *J. Biol. Chem.* **1990**, *265*, 14382−14387.
(49) Tahirov, T. H.; Misaki, S.; Meyer, T. E.; Cusanovich, M. A.; Higuchi, Y.; Yasuoka, N. *J. Mol. Biol.* **1996**, *259*, 467−479.
(50) Shibata, N.; Iba, S.; Meyer, T. E.; Bartsch, R. G.; Cusanovich, M. A.; Morimoto, Y.; Higuchi, Y.; Yasuoka, N. *J. Mol. Biol.* **1998**, *284*, 751−760.
(51) Wirtz, M.; Oganesyan, V.; Zhang, X.; Studer, J.; Rivera, M. *Faraday Discuss.* **2000**, *116*, 221−234.
(52) Stellwagen, E. *Nature* **1978**, *275*, 73−74.
(53) Kassner, R. J. *J. Am. Chem. Soc.* **1973**, *95*, 2674−2677.
(54) Kassner, R. J. *Proc. Natl. Acad. Sci. U.S.A.* **1972**, *69*, 2263−2167.

2_{c554}, heme 4_{HAO}), each heme of cyt c_{554} and HAO coordinates to one His (proximal) in the sequence −C−X−Y−C−H− and one His (distal) that is not in this sequence. This structural homology extends to orientations of the imidazole planes relative to the respective hemes. With the exception of the distal His102 of heme 1_{c554}, each imidazole plane of a homologous heme has the same orientation. As noted in the structural work,[12,13] His102 coordinates as N_δ to the iron and is the first known heme protein to show such coordination.

Model heme complexes and peptide assemblies have shown that an N_δ axial imidazole coordination to a heme results in a steric interaction between the C_β atom of the imidazole and the porphyrin ring.[30,39,55−58] This interaction results in lengthening of the Fe−N_δ bond. The steric interaction is lessened by a ruffling of the porphyrin ring and a perpendicular orientation of the two axial imidazole planes. These effect are observed for the N_δ His102 coordination to heme 1_{c554}. The Fe−N_δ bond (2.08 Å) is long, the porphyrin plane shows increased distortion from planarity, and the axial imidazole planes (His102/His15) are perpendicular.[13] These two effects should result in an overall positive shift of E_m for heme 1_{c554} relative to heme 3_{HAO}, as is in fact observed.[59] Mitigating contributions to an overall positive shift are an H-bond between axial His102 and Glu126 (2.7 Å) of heme 1_{c554} and a higher solvent exposure compared with heme 3_{HAO}, both of which should contribute to a lower reduction potential. The homologous His99 at heme 3_{HAO} has no nearby polar residues. Both heme 1_{c554} and heme 3_{HAO} show similar H-bonding to propionates. The E_m of the homologous heme 1_{SSC} is significantly lower, presumably because of the greater solvent accessibility of this heme.

The distal His179 of heme 3_{c554} is H-bonded to Glu180 (2.7 Å), whereas the homologous His323 of heme 5_{HAO} has no H-bonds. This should give a negative shift in E_m for heme 3_{c554}. Both propionates of heme 3_{c554} are H-bonded (His197, 2.9 Å; His182, 2.7 Å), whereas the propionates of heme 5_{HAO} have no H-bonds. This should give a positive shift in E_m. The solvent accessibility (low) and axial His coordination for the two hemes are similar. Thus, we expect and observe an overall negative shift in E_m of heme 3_{c554} versus heme 5_{HAO}. However, we note without explanation that the magnitude of this shift (∼150 mV) is perhaps too large to be attributed to one H-bond. The homologous heme 2_{SSC} and heme 2_{NiR} both have significant solvent exposure and should have relative lower potentials. This is observed for SSC but not for NiR.

The distal His27 of heme 4_{c554} is H-bonded to a backbone carbonyl of Ala177 (2.8 Å), whereas heme 6_{HAO} has no polar residue near its axial histidines. Heme 4_{c554} is more solvent exposed than heme 6_{HAO}. Thus, the lower potential of heme 4_{c554} may be attributed to these two effects.[52−54] The axial histidines of the two hemes have similar coordination, and both hemes have H-bonds to their respective propionates.

Finally, the two hemes which appear 5-coordinate in the crystal structure are heme 2_{c554} (+47 mV) and heme 4_{HAO} (−260 mV). We have concluded previously that heme 4_{HAO} is low-spin,[29,46] which we now assert is due to the presence of a hydroxide ligand at the sixth coordination site of heme 4_{HAO}. The low-spin state and nearly 300 mV decrease in potential of heme 4_{HAO} are consistent with the binding of an anionic ligand to the sixth coordination site, such as hydroxide.

Rationalization of Cyt c_{554} Kinetic Data. We have demonstrated here that the thermodynamic final state of cyt c_{554} reduced by hydrazine/HAO has two hemes reduced. As with previous stop-flow kinetic studies of the reduction of cyt c_{554} following mixing with HAO and an excess of hydroxylamine or hydrazine, we also observed a two-electron reduction of cyt c_{554}. These two electrons were observed to reduce cyt c_{554} in two one-electron transfer processes, at rates of $k_1 > 300\ s^{-1}$ and $k_2 = 30\ s^{-1}$.[7] Importantly, the first reduction was assigned to heme 2, and thus, the second reduction process, to one of the low-spin hemes. Hemes 1 and 2 are both at the surface of cyt c_{554}, but at opposite sides of the protein, approximately 20 Å apart. Our assignments determine that these are the two most positive hemes. There are two schemes which can rationalize the observed rates with these assignments.

For the first scheme, we assume that cyt c_{554} binds to HAO such that heme 1_{HAO} (donor) is near to heme 2_{c554} (acceptor). Thus, the fast reduction of heme 2_{c554} (+47 mV) is followed by the slower reduction of heme 4_{c554} (−276 mV). The two hemes are in electronic contact; thus, the main factor determining the reduction rates is the free energies of the hemes, rather than the distance dependence. The relative rates of electron transfer can be calculated using the Marcus relation, $\log k_{et} = A - 3.1(\Delta G + \lambda)^2/\lambda$.[60,61] We assume that the reorganization energies are $\lambda = 0.7$ eV for both processes and that the term, A, involving the cofactor separation is the same for both processes. From this relation, we calculate a ratio $k_1/k_2 = 9$,[62] which agrees with the ratio observed experimentally.[7]

A concern with the previously mentioned scheme is that a crystallographic analysis of the surface charge of HAO and cyt c_{554} suggests that cyt c_{554} docks to HAO with heme 1_{c554} close to heme 1_{HAO}. In the second scheme, the first electron transfer occurs from heme 1_{HAO} to heme 1_{c554}. Presumably, the transfer process is vectorial, and the low-spin hemes of cyt c_{554} are transiently reduced to finally reduce the more positive heme 2_{c554}. Since heme 2_{c554} is observed to be reduced, the other reducing equivalent is in the heme 1_{c554}. An explanation of the kinetic data within this scheme requires that the reduction of the low-spin hemes of cyt c_{554} occurs faster than the reduction of heme 2_{c554} ($k_1 > 300\ s^{-1}$) and thus is not observable. The slower observed process ($k_2 = 30\ s^{-1}$) attributed to the reduction of a low-spin heme in cyt c_{554} is in this case an artifact of low-spin heme reduction in HAO, a possibility first suggested in kinetic work.[7] In Mössbauer spectra of cyt c_{554} poised with hydroxylamine and a catalytic amount of HAO, we observe a

(55) Choma, C. T.; Lear, D. J.; Nelson, M. J.; Dutton, P. L.; Robertson, D. E.; DeGrado, W. F. *J. Am. Chem. Soc.* **1994**, *116*, 856−865.
(56) Geiger, D. K.; Lee, Y. L.; Scheidt, W. R. *J. Am. Chem. Soc.* **1984**, *106*, 6339−6343.
(57) Hatano, K.; Safo, M. K.; Walker, F. A.; Scheidt, W. R. *Inorg. Chem.* **1991**, *30*, 1643−1650.
(58) Scheidt, W. R.; Kirner, J. L.; Hoard, J. L.; Reed, C. A. *J. Am. Chem. Soc.* **1987**, *109*, 1963−1968.
(59) Reference 13 states that the orientation of the N_δ His102 of heme 1_{c554} does not change relative to that of the N_ϵ His99/His176 of heme 3_{HAO}. However, we do find a change between the two structures. The imidazole planes of the later two histidines nearly align themselves along the plane through two pyrrole nitrogens of the porphyrin, whereas the imidazole plane of His102 in cyt c_{554} nearly bisects the planes drawn through the pyrrole nitrogens and is perpendicular to axial His15.

(60) Page, C. C.; Moser, C. C.; Chen, X.; Dutton, P. L. *Nature*, **1999**, *402*, 47−52.
(61) Moser, C. C.; Dutton, P. L. *Biochim. Biophys. Acta* **1992**, *1101*, 171−176.
(62) The potential of heme 1_{HAO} is −412 mV, −265 mV, or +288 mV. We suspect it has one of the more negative values, given the extensive solvent exposure of heme 1. We have assumed the value −412 mV for the calculation.

complete reduction of heme 1_{c554} and 40% reduction of high-spin heme 2_{c554}. This causes complications in the interpretation of both the Mössbauer and EPR spectra of this sample, and we therefore address only the hydrazine/HAO reduction results in this paper. Nevertheless, it is clear that hydroxylamine/HAO reduction results in a different equilibrium state of cyt c_{554} than hydrazine/HAO reduction, suggesting that heme 1_{c554} is reduced prior to heme 2_{c554}. This result and the crystallographic analysis thus favor the second scheme.

Conclusion

Cyt c_{554} functions only in electron transport, since the 5-coordinate heme cannot accept ligands. The specific potentials of the hemes are now assigned. The magnitudes of the potentials relative to the homologous hemes of HAO can be rationalized by axial ligand differences. These axial ligand differences, in turn, impart significant changes to the spectroscopy of the proteins. The four hemes of cyt c_{554} are exchange-coupled in two independent pairs, similar to that observed in HAO. This work provides important determinants for further kinetic and enzymatic studies of HAO/cyt c_{554} biochemistry and a more general ability to interpret spectroscopic observations from complicated multiheme proteins.

Acknowledgment. This work was supported from grants by NIH 49970 (M.P.H.) and NSF/MCB 0093447 (A.B.H.). We thank Caleb Culver for help in acquiring the Q-band data and microwave cavity construction.

JA020922X